Published in final edited form as:
Gastroenterology. 2013 November ; 145(5): 1045–1054. doi:10.1053/j.gastro.2013.07.011.

Dual Oxidases Control Release of Hydrogen Peroxide by the Gastric Epithelium to Prevent *Helicobacter felis* Infection and Inflammation in Mice

Helmut Grasberger[1], **Mohamad El-Zaatari**[1], and **Juanita L. Merchant**[1,2]

[1]Department of Internal Medicine, Division of Gastroenterology, University of Michigan, Ann Arbor, MI 48109

[2]Department of Molecular and Integrative Physiology, University of Michigan, Ann Arbor, MI 48109

Abstract

Background & Aims—Dual oxidases (DUOX) are conserved NADPH oxidases that produce H_2O_2 at the epithelial cell surface. The DUOX enzyme comprises the DUOX and DUOXA (DUOX maturation factor) subunits. Mammalian genomes encode 2 DUOX isoenzymes (DUOX1–DUOXA1 and DUOX2–DUOXA2). Expression of these genes is upregulated during bacterial infection and chronic inflammatory diseases of the luminal gastrointestinal tract. The roles of DUOX in cellular interactions with microbes have not been determined in higher vertebrates.

Methods—Mice with disruptions of *Duoxa1* and *Duoxa2* genes (*Duoxa*$^{-/-}$ mice) and control mice were infected with *Helicobacter felis* to create a model of *Helicobacter pylori* infection—the most common human chronic infection.

Results—Infection with *H felis* induced expression of Duox2 and Duoxa2 in the stomachs of wild-type mice, and DUOX protein specifically localized to the apical surface of epithelial cells. *H felis* colonized the mucus layer in the stomachs of *Duoxa*$^{-/-}$ mice to a greater extent than in control mice. The increased colonization persisted into the chronic phase of infection and correlated with an increased, yet ineffective, inflammatory response. *H felis* colonization was also increased in *Duoxa*$^{+/-}$ mice, compared with controls. We observed reduced expression of the H_2O_2-inducible *katA* gene in *H felis* that colonized *Duoxa*$^{-/-}$ mice, compared with that found in controls (P=.0002), indicating that Duox causes oxidative stress in these bacteria. In vitro, induction of oxidative defense by *H felis* failed to prevent a direct bacteriostatic effect, at sustained levels of H_2O_2 as low as 30 μM.

Correspondence: Helmut Grasberger, University of Michigan, BSRB, Rm2468, 109 Zina Pitcher Place, Ann Arbor, MI 48109, Phone: +1-734-936-6363, Fax: +1-734-763-4686, hgrasber@gmail.com.

Author contributions:
HG: study concept and design; data acquisition and analysis; wrote manuscript; obtained funding
MEZ: acquisition of data; review of manuscript
JLM: obtained funding; study design; review of manuscript

Disclosures:
The authors have nothing to disclose.

Conclusions—Based on studies of *Duoxa*$^{-/-}$ mice, the DUOX enzyme complex prevents gastric colonization by *H felis* and the inflammatory response. These findings indicate the non-redundant function of epithelial production of H_2O_2 in restricting microbial colonization.

Keywords

dual oxidase; mouse model; mucosal immunity; gastritis

Introduction

Studies in invertebrates have been seminal in deciphering innate immune defense mechanisms that are conserved in vertebrates including humans [1]. Invertebrate gut epithelial immune responses rely mainly on two types of complementary and synergistic molecular effectors that restrict proliferation of microorganisms: antimicrobial peptides and reactive oxygen species. The latter are released by dual oxidase (DUOX), a hydrogen peroxide (H_2O_2) generating membrane-associated NADPH oxidase [2].

Knockdown of *duox* in the *Drosophila* gut leads to a severe host defense defect against a broad spectrum of pathogens [3,4]. Studies in *duox* deficient *C. elegans* confirmed that H_2O_2 release from mucosal surfaces is an ancient defense mechanism predating the evolution of the oxidative burst in specialized immune cells [5]. More recently, knockdown of zebrafish *duox* was shown to increase the intracellular bacterial load of larvae infected with enteric *Salmonella* suggesting that an antibacterial function of DUOX is conserved in lower vertebrates [6].

The functional DUOX enzyme complex is a heterodimer formed by association of two multipass transmembrane proteins, DUOX and DUOXA (DUOX maturation factor) (Fig. 1A). Mammalian genomes encode two DUOX isoenzymes, each representing a heterodimer of distinct DUOX and DUOXA subunits (i.e., DUOX1/DUOXA1 and DUOX2/DUOXA2) [7–9] (Fig. 1B). Both DUOX enzymes are H_2O_2-producing calcium-stimulated NADPH oxidases, but differ in transcriptional regulation. The conserved expression of DUOX2 throughout the luminal gastrointestinal (GI) tract of vertebrates, including humans,[10] suggests it may confer a crucial evolutionary advantage. *DUOX2* and *DUOXA2* have been identified among the highest induced genes in Crohn's disease [11,12], irritable bowel syndrome [13], and infectious diseases, such as *Helicobacter pylori*-associated gastritis [14]. Despite the potential importance of this system in the pathophysiology of common human diseases, its role in mucosal defense has not been explored in any higher vertebrates *in vivo*.

Deletion of both *Duoxa* genes produces mice lacking the expression of functional DUOX enzymes (*Duoxa*$^{-/-}$ mice) [15] (Fig. 1B). We have now used this line of mice to investigate the role of DUOX-generated H_2O_2 in the mucosal defense against *Helicobacter felis* (*Hf*), a well-established model for *H. pylori* infection in humans, the most common chronic bacterial infection [16]. Our results provide a paradigm for the role of DUOX in controlling microbial populations in the juxtamucosal mucus layer.

Results

Helicobacter Infection Induced DUOX2 Expression in the Gastric Epithelium

Wild type mice kept in a specific-pathogen free environment expressed both *Duox2* and *Duoxa2*, but not *Duox1* and *Duoxa1* mRNA in the stomach (average threshold cycle [ct] in realtime PCR: 25.5 for *Duox2*; 28.5 for *Duoxa2*; 38.3 for *Duox1*; >40 for *Duoxa1*). The

predominant expression of the DUOX2 isoenzyme in the murine stomach is consistent with the GI tract expression in other mammals [10].

In wild type mice, infection with *Hf* acutely induced *Duox2* and *Duoxa2*. Nine days post infection, induction of *Duoxa2* and *Duox2* was 6.9 fold (P=.008) and 3.2-fold (P=.06), respectively (Fig. 1C–D). The expression of both genes remained elevated at 6 months post infection. By immunofluorescence, DUOX protein was barely detectable in control animals (Suppl. Fig. 1A–B) but showed strong multifocal expression in the gastric mucosa of *Hf* infected mice (Fig. 1F). Expression in infected mice was limited to epithelial cells and absent in stromal cells.

In *Duoxa*$^{-/-}$ mice, no *Duoxa2* transcripts spanning the targeted deletion were detected as expected (Fig. 1C), but baseline *Duox2* expression levels did not differ from wild type controls. Induction of *Duox2* mRNA by *Hf* infection was higher than in infected wild type animals (Fig. 1D) suggesting a stronger activation of signaling pathways that induce *Duox2* expression. Lack of DUOXA heterodimerization partners prevents ER-exit of DUOX proteins [15], a finding confirmed by absence of apical targeting of DUOX proteins in gastric epithelium of *Duoxa*$^{-/-}$ animals (Fig. 1E). To directly assess the functional activity of DUOX proteins, isolated gastric glands were tested for the ability to release H_2O_2 into the medium. Glands isolated from wild type animals generated over 4-fold higher extracellular H_2O_2 levels compared to those from *Duoxa*$^{-/-}$ littermates (Fig. 1F). Impaired H_2O_2 generation in *Duoxa*$^{-/-}$ mice was observed in *Hf* infected animals as wells as mock-infected controls. These data indicate that DUOX proteins are a major source of epithelial derived extracellular H_2O_2 in the murine stomach.

Lack of Functional DUOX Enzymes Increased Mucosal Colonization with *Helicobacter*

To examine whether DUOX activity affects gastric colonization and persistence of *Hf*, we measured colonization levels by semiquantitative realtime PCR. In *Duoxa*$^{-/-}$ animals, colonization levels were higher during both the acute and chronic phases of infection (Fig. 2A). Immunofluorescent detection of *Hf* revealed that colonization was limited to the mucus layer in both *Duoxa*$^{-/-}$ and wild type mice (Fig. 2B). There were no differences in gastric acidity, the number of parietal cells or the expression of H^+/K^+-ATPase subunit genes that could have affected *Hf* colonization (Fig. 2C, Suppl. Fig. S2) [17]. Also, overall morphology of the gastric glands (by H&E staining) and mucus pattern (by Alcian Blue/PAS staining) were both indistinguishable between *Duoxa*$^{-/-}$ and wild type controls (data not shown).

Lack of DUOX Activity Lead to Exacerbated Acute and Chronic *Helicobacter*-Induced Gastritis

The acute phase of *Hf*-induced gastritis was characterized by diffuse polymorph- and mononuclear infiltrates in the subglandular region. In infected *Duoxa*$^{-/-}$ mice, infiltrates were more widespread than in wild type controls and frequently displaced the lower portion of the glands (Fig. 3A). In accordance, mRNAs for acute inflammatory markers, such as interleukin-β, interferon-γ, the chemokine CXCL1 (a murine interleukin-8 equivalent), and TNF-α were expressed at a higher level in the stomach of infected *Duoxa*$^{-/-}$ mice compared to infected controls (Fig. 3B–C; Suppl. Fig. S3A–B).

In the chronic phase of infection, the gastric mucosa of *Duoxa*$^{-/-}$ mice showed more extensive diffuse mononuclear infiltrates and higher numbers of lymphoid follicles (Fig. 4A–D). The chemokine CXCL13 (also known as B cell chemoattractant-1; BCA-1) dictates homing and motility of B-cells in lymphoid tissue, and its induction in chronic *H. pylori* gastritis is involved in the formation of lymphoid follicles and gastric lymphomas of the MALT type [18]. In *Duoxa*$^{-/-}$ mice, the infection-induced expression of *Cxcl13* and the B-cell

marker *Cd19* was 3.1 and 4.1-fold, respectively, higher than in wild type controls, in agreement with the histopathological finding of increased follicle development in the gastric mucosa of *Duoxa*$^{-/-}$ mice (Fig. 4E; Suppl. Fig. S3C). During *Helicobacter* infection, T-helper 17 (Th17) cells secrete large amounts of interleukin-17A that acts on a variety of target cells, including epithelial cells, to upregulate the production of neutrophil chemotactic factors [19]. In *Duoxa*$^{-/-}$ mice, average *IL17a* expression at 6 months was 4.1-fold higher than in wild type controls (Fig. 4F). Overall, *Helicobacter*-induced Th1, Th17, and B-cell responses showed identical patterns in *Duoxa*$^{-/-}$ and control mice, but were far more robust in *Duoxa*$^{-/-}$ mice. The expression of proinflammatory markers positively correlated with the level of colonization by *Hf* (Suppl. Fig. S4), consistent with the concept that *Hf*-induced inflammation is a response to shed antigens or secreted virulence factors [20]. The pivotal role of DUOX in limiting *Hf* infection and gastritis was underscored by the apparent haploinsufficiency of heterozygous *Duoxa*$^{+/-}$ animals: their mucosal colonization levels and inflammation scores were intermediate to wild type and homozygous *Duoxa*$^{-/-}$ animals (Fig. 3, 4; Suppl. Fig. S3, S4).

Hf Colonizing the Mucosa of *Duoxa*$^{-/-}$ Animals Expressed Lower Levels of H_2O_2-Inducible *katA*

It is well established that exposure of microbes to reactive oxygen species can modulate redox-sensitive signaling molecules and transcription factors, leading to adaptive responses, and changes in virulence or viability [21,22]. While it is not feasible to directly measure the effective H_2O_2 concentration *Hf* is exposed to in its physiological niche *in vivo*, differential exposure of *Hf* to H_2O_2 should be reflected in differences in H_2O_2-responsive gene expression. *Helicobacter* catalase is expressed at the cell surface and its only known function is the degradation of exogenous H_2O_2 [23]. The single catalase gene of *Hf* (*katA*) [24] is therefore a prime candidate for redox-sensitive regulation by DUOX-generated H_2O_2. Analogous to *katA* of *H. pylori* [25], *katA* of *Hf* was indeed induced by a single H_2O_2 bolus (Fig. 5A). No induction was observed for *flaB*, a gene previously employed as a housekeeping gene in oxidative stress response studies [26]. Importantly, in both acute and chronic infection, *Hf* colonizing control animals expressed higher *katA:flaB* ratio compared to *Hf* found in *Duoxa*$^{-/-}$ mice (Fig. 5B). These results imply that the rate of H_2O_2 production by the activated DUOX system is sufficient to modulate redox sensitive gene expression in *Hf* colonizing the overlaying mucus layer.

Micromolar Concentrations of H_2O_2 have a Powerful Bacteriostatic Effect on *Hf in vitro*

Our results showed that inactivation of the DUOX system lead to increased bacterial colonization, which positively correlated with the inflammatory response in the *Hf* infection model. In addition, DUOX activity was associated with oxidative stress response in colonizing *Hf* in vivo. We thus hypothesized that DUOX-generated H_2O_2 acts as a direct suppressor of *Hf* colonization. To provide evidence for this concept, we assessed whether H_2O_2 at low concentrations would be sufficient to limit *Hf* proliferation. H_2O_2 (15 μM to 1 mM) was stable in sterile culture medium, but disappeared within one hour with the presence of *Hf* in the medium indicating that the bacteria efficiently scavenged H_2O_2 (Fig. 6C and data not shown). To test whether direct H_2O_2 addition could still inhibit proliferation of bacteria in the ensuing culture, bacterial DNA and intracellular ATP level were determined after culture under microaerophilic conditions. We found that a single H_2O_2 bolus as low as 100 μM was sufficient to suppress *Hf* proliferation under these conditions (Fig. 6A–B).

To substantiate these findings and better mimic the situation of sustained H_2O_2 production found *in vivo*, we challenged the H_2O_2 scavenging activity of *Hf* with increasing amounts of glucose oxidase as an H_2O_2 source. In this system, the H_2O_2 level is directly proportional to

the ratio of glucose oxidase activity to bacterial H_2O_2 scavenging activity. As expected, loss of proliferation was observed when the initial H_2O_2 concentration exceeded a critical threshold, whereas in cultures with lower initial H_2O_2 equilibrium, *Hf* was able to outgrow the enzymatic H_2O_2 source. Under the culture conditions employed, the critical threshold for sustained H_2O_2 exposure was approximately 30 μM (Fig. 6D–F), a physiologically relevant concentration in extracellular compartments [27].

Discussion

Studies in invertebrates and zebrafish larvae have indicated a crucial role of DUOX enzymes in host defense within the luminal GI tract [3,6,28]. The inducible production of hydrogen peroxide functions as a second effector arm of epithelial innate immunity, complementary and synergistic to the better characterized antibacterial peptide system [1]. However, up until now, only the role of the latter has been analyzed in higher vertebrate species in vivo.

Here, using *Helicobacter* infection in *Duoxa*$^{-/-}$ mice as a model system, we demonstrate for the first time a nonredundant function of the DUOX system in mammalian GI immunity. Our results provide evidence that H_2O_2 released by DUOX at the apical surface of the gastric epithelium suppresses proliferation of *Helicobacter* in the overlying mucus layer. The identification of DUOX-generated H_2O_2 as a pivotal host factor in the homeostatic interaction with *Helicobacter* is consistent with prior studies showing the failure of oxidative stress resistance mutants to persist in the murine stomach [29,30]. In mice lacking active DUOX enzymes, *Hf* was able to colonize at a higher level but did not escape from its normal niche within the mucus layer. Shedding of bacterial antigens and secretion of virulence factors trigger *Hf*-induced gastritis, which, as expected from the increased bacterial load, was more severe in *Duoxa*$^{-/-}$ animals. Furthermore, consistent with a primary defect in cell-autonomous epithelial defense, elevated colonization levels in *Duoxa*$^{-/-}$ persisted in the chronic phase of infection despite a stronger adaptive immune response. The pivotal role of DUOX in host defense against *Hf* was underscored by the severity of the *Hf*-induced phenotype in heterozygous mice (*Duoxa*$^{+/-}$), which was intermediate to wild type and *Duoxa*$^{-/-}$ mice suggesting haploinsufficieny. This observation is in contrast to the normal thyroid hormone synthesis in *Duoxa*$^{+/-}$ [15], and implies that the GI epithelium expressing almost exclusively the DUOX2 isoenzyme, has a lower capacity to compensate partial DUOX defects than the thyroid epithelium expressing both DUOX isoenzymes constitutively.

The release of H_2O_2 from the luminal surfaces of the GI tract and its degradation within the mucus layer is expected to generate a rapidly dissipating H_2O_2 gradient. In fact, we were unable to detect significant H_2O_2 release from the luminal mucus surface ex vivo suggesting complete consumption of epithelial produced H_2O_2 within the mucus layer (data not shown). It remains to be shown whether H_2O_2 released into the mucus is primarily decomposed into H_2O and O_2, or whether it drives peroxidative formation of more stable oxidants, such as, HOSCN and HOCl with powerful microbicidal activity [31]. Nevertheless, since the enzymatic activity of stimulated DUOX is comparable to the activated leukocyte NADPH oxidase [32], the H_2O_2 challenge encountered by microbes close to the epithelium should be substantial. At least in the stomachs of gerbils, the currents recorded with H_2O_2 sensitive microsensors indicate a greatly increased rate of H_2O_2 release into the juxtamucosal mucus layer following infection with *H. pylori* [33]. *Hf* almost exclusively occupies a defined niche between 5–20 μm from the epithelial surface [34], a restriction dictated by the pH gradient within the mucus layer [35]. These constraints on the vertical distribution of *Hf* may be critical for the efficient exposure to DUOX-generated H_2O_2. That DUOX-generated H_2O_2 indeed altered redox signaling in *Hf in vivo* was substantiated by significant higher *katA* expression in *Hf* colonizing wild type mice compared to those from

Duoxa$^{-/-}$. As we have shown here, growth of *Hf* is highly susceptible to H_2O_2, which exerts a bacteriostatic effect at low micromolar concentrations *in vitro*.

That low concentrations of exogenous H_2O_2 can affect bacterial redox signaling has been demonstrated previously for other catalase positive bacteria. For instance, in *E. coli*, 5 μM of environmental H_2O_2 corresponding to an intrabacterial level just above 100 nM, is sufficient to activate the redox sensor OxyR that controls the adaptive responses to H_2O_2 stress, including induction of catalase [36]. In *Campylobacter jejuni* a single H_2O_2 bolus of 10 μM is sufficient to suppress polysaccharide capsule synthesis without direct microbicidal effects [37]. In our in vitro system, sustained exposure to 30 μM H_2O_2 was sufficient to also interfere with bacterial growth. These results are similar to those obtained in studies of *E. coli* using continuous H_2O_2 infusion where profound growth retardation was observed between 25–50 μM, and complete bacteriostasis at 100 μM H_2O_2 [38]. It should be stressed that the antimicrobial effect of a single H_2O_2 bolus depends on the bacterial density, and the apparent tolerance to high millimolar H_2O_2 boli in other studies using concentrated cell suspensions does not seem to reflect the true bacteriostatic potential of a sustained H_2O_2 flux [22].

While this study illustrates how DUOX controls a noninvasive pathogen colonizing the mucus layer, we expect DUOX to be effective against a broad spectrum of pathogens including those that penetrate the inner mucus layer and make direct contact with the epithelial surface. In the latter scenario, the host defense function of DUOX could be further enhanced by recruitment of the DUOX enzyme complex to the site of bacterial contact, as shown in response to *Listeria monocytogenes* and *Campylobacter jejuni* infection in vitro [37,39]. Conceivably, such targeting of DUOX should generate a high level H_2O_2 flux across the bacterial membrane and could explain the DUOX-mediated protection in *Drosophila* and zebrafish larvae from the highly invasive pathogen *Salmonella* Typhimurium [3,6].

Although not specifically addressed by our study, DUOX-generated H_2O_2 may well have additional effects on the immune response beyond its antimicrobial properties. H_2O_2 is now widely recognized as an important signal messenger of various intracellular signaling pathways [40]. Although intracellular H_2O_2 signaling is spatially restricted [41], there is evidence from in vitro systems that DUOX-generated H_2O_2 may enter producing or neighboring cells, e.g. facilitated by specific aquaporins [42], and oxidize redox-sensitive signaling molecules in the vicinity of the plasma membrane. There is also a possibility that DUOX generated H_2O_2 can provide a signal for nonepithelial cells relevant in the immune response. For instance, epithelial wounding in zebrafish larvae or *Drosophila* embryo epidermis activates DUOX at the wound margin to release H_2O_2 [43,44], with the resulting tissue-scale H_2O_2 gradient attracting immune cells to migrate to the epithelial lesion. In addition, there is evidence that DUOX activity stimulates migration of epithelial cells during wound closure [45,46]. Whether DUOX plays such roles in a mammalian system in vivo will have to be tested in a model that, unlike *Hf* infection, induces epithelial injury.

Taken together, our study provides in vivo evidence for a nonredundant function of DUOX-generated H_2O_2 as epithelial immune effector in the luminal GI tract. In our chronic infection model, loss of active DUOX enzymes led to increased mucosal colonization and exacerbated, yet futile, chronic inflammatory response. The subunits of the DUOX2 isoenzyme have been identified among the highest induced genes in Crohn's disease [11,12], irritable bowel syndrome [13], and infectious diseases [14,47]. It remains to be shown whether loss of DUOX activity will also exacerbate other infectious or chronic inflammatory conditions of the luminal GI tract in which *DUOX* was found to be activated.

Materials and Methods

Animals

The generation of *Duoxa*$^{-/-}$ mice has been described previously [15]. All animals used were females in a pure 129S6 genetic background. Within infection experiments, average body weight and age did not differ between the different genotype/treatment groups. Animals were group-housed (3–5 animals/cage; mixed genotypes) in microisolator cages under specific-pathogen-free conditions. Food and water were supplied ad libitum, with the latter including a supplemental dose of L-thyroxine to maintain euthyroidism of *Duoxa*$^{-/-}$ mice [15]. Prior to necropsy, mice were fasted overnight on wire mesh with free access to water. All studies were approved by the University of Michigan Institutional Animal Care and Use Committee (PRO-00004497).

Hf culture and infection

See Supplementary Methods section.

Tissue dissection

See Supplementary Methods section.

H_2O_2 release of isolated mouse gastric glands

The glandular portions of the stomachs were excised and everted by cutting along the lesser curvature. The rinsed stomachs were kept in oxygenated digestion medium (Dulbecco's Modified Eagle Medium, 20 mM Hepes pH 7.4, 10 μg/ml soybean trypsin inhibitor, 0.2% bovine serum albumin, 100 U/ml penicillin, 100 μg/ml streptomycin, 0.25 μg/ml amphotericin B). For collagenase treatment, stomachs were placed in 10 ml fresh digestion medium containing 1 mg/ml collagenase (type XI; >1200 collagenase digestion units/mg protein; Sigma, St. Louis, MO) and incubated at 37°C in a shaking incubator (130 rpm) for 40 minutes. The partially digested stomachs were held with forceps and shaken in DMEM/F12 medium supplemented with 0.5 mM dithiothreitol to liberate gastric glands. The resulting suspension was passed through a 100 μm nylon filter mesh. The filtrate was sedimentated (30 g for 4 min) and gently washed thrice each in digestion buffer and Krebs-Ringer-Hepes buffer (KRH; 124 mM NaCl, 5 mM KCl, 1.25 mM $MgSO_4$, 1.45 mM $CaCl_2$, 1.25 mM KH_2PO_4, 25 mm Hepes pH 7.4, 8 mM D-glucose, and 0.5 g/L BSA) to remove isolated cells. In the final preparations, >95% of the cells were found in multi-cellular clusters. Cell viability was confirmed by trypan blue exclusion. The glands from each stomach were incubated for one hour in KRH with or without 100 U/ml catalase (Sigma). H_2O_2 accumulation in the supernatant was determined using the Amplex Red/horseradish peroxidase (HRP) assay (Life Technologies). Catalase-inhibitable relative fluorescence units were converted to H_2O_2 concentrations using standards prepared in KRH. Gland pellets were lysed in T-PER Tissue Protein Extraction Reagent and protein content determined using the BCA assay (Thermo Fischer Scientific, Rockford, IL).

Histology and morphometric analysis

Serial 4 μm sections of formalin-fixed paraffin-embedded samples were stained with hematoxylin and eosin (H&E). For histopathological evaluation of gastric inflammation, microscopic fields at 200× magnification were scored as described by Eaton et al. [48]. For each animal, scores represent the percentage of the fields displaying gastric gland displacement or lymphoid aggregates, respectively.

Immunostaining of tissue sections

For staining of frozen sections, thawed 8 μm sections were fixed again in 4% freshly prepared formaldehyde for 10 min, washed twice in PBS, and then blocked with 20% donkey serum in PBS. Primary antibodies used were a pan-DUOX antiserum [8] or normal rabbit IgG (control; Santa Cruz Biotechnology, Santa Cruz, CA), an anti-*H. pylori* serum (Covance, Princeton, NJ), and rat anti-E-cadherin (Invitrogen). The staining was developed using Alexa Fluor-conjugated secondary antibodies (Life Technologies) and DNA counterstained with DAPI. Mucins were visualized using biotinylated *Ulex Europaeus* agglutinin 1 (UEA-1; Vector Laboratories, Burlingame, CA) with Texas-Red conjugated anti-biotin antibodies (Jackson ImmunoResearch Laboratories, West Grove, PA).

Real-time reverse transcription PCR (RT-qPCR)

See Supplementary Methods section.

Exposure of *Hf* to H_2O_2 in vitro and proliferation assays

Hf from a mid-log culture were washed and resuspended in phenol red-free RPMI-1640 medium supplemented with 2% heat inactivated FBS. Although RPMI/FBS did not meet the nutritional requirements for longterm culture of *Hf* [49], it supported limited proliferation within the first 24 hours (Fig. 5A). For bolus treatment, H_2O_2 from a 3% stock solution (880 mM) was diluted into culture medium that had been equilibrated in a microaerophilic atmosphere followed by addition of washed bacteria at $3.2 \cdot 10^6$/ml. Culture was then performed for 18 hours.

For sustained H_2O_2 exposure, bacterial dilutions ($1.6 \cdot 10^6$/ml) were prepared in 16 ml phenol red-free DME/F12/2% FBS in vented T150 flasks that had been equilibrated in a microaerophilic atmosphere. Glucose oxidase (GOX; Sigma) was serially diluted in glucose-free phosphate buffer and mixed with the cultures (final: 2.5–40 mU/l; K_M=9.8 mM; [D-glucose]=17.15 mM). In control experiments, 400 U/l catalase was added to the flasks prior to the addition of GOX. Samples of the cultures were obtained immediately after setting-up the reaction (t=0 h) and following 24 h culture (t=24 h). The initial equilibrium [H_2O_2] was derived from the y-intercept (t=0 h) of the kinetics of resorufin generation in the Amplex Red/HRP assay with H_2O_2 standards diluted in PBS (note that $k_{HRP} \gg k_{catalase}$). Repeat measurements confirmed that the initial steady state [H_2O_2] had been reached at less than 5 min following addition of GOX at the highest dilution. Within the linear range of the assay, [H_2O_2] was directly proportional to the ratio of [*Hf*] versus [GOX]. Values >10 μM were derived by linear extrapolation. Equilibrium [H_2O_2] at t=24 h had typically either shifted close to background level of the medium (growing cultures suppressing [H_2O_2]) or exceeded the range of the assay (bacteria inactivated by accumulating H_2O_2).

Intracellular ATP levels of bacteria were determined using a luciferase-based method (BacTiter-Glo Microbial cell viability assay kit; Promega, Fitchburg, WI). To determine the relative amount of bacterial DNA, cultures were diluted 1:5 in 200 mM Tris-HCl pH 8.0/50 mM EDTA containing SYBR Green I (1:2000 dilution of a 10,000× stock solution), and the fluorescence signal (ex/em, 485/535 nm) recorded. Values were corrected for the background fluorescence of sterile medium.

Statistics

The Mann-Whitney *U* test or unpaired Student *t* test were used for comparison of two groups. For multiple comparisons, data were analyzed using the Kruskal-Wallis test or one-way analysis of variance following log-transformation. Multiple comparison adjusted *P* values for pairwise comparisons were then calculated using Dunn's multiple comparison test

or Tukey's post-hoc test, respectively. Data were analyzed and plotted using GraphPad Prism software, version 5 (San Diego, CA). *P* values <.05 were considered significant.

Supplementary Material

Refer to Web version on PubMed Central for supplementary material.

Acknowledgments

We thank X. De Deken and F. Miot for providing the DUOX antiserum, and M. Saqui-Salces for critical review of the manuscript. This study was supported by NIH grant DK55732 and a Pilot and Feasibility Grant of the University of Michigan Gastrointestinal Peptide Research Center (P30 DK034933).

References

1. Lemaitre B, Hoffmann J. The host defense of Drosophila melanogaster. Annual review of immunology. 2007; 25:697–743.
2. Bae YS, Choi MK, Lee WJ. Dual oxidase in mucosal immunity and host-microbe homeostasis. Trends in immunology. 2010; 31:278–287. [PubMed: 20579935]
3. Ha EM, Oh CT, Bae YS, et al. A direct role for dual oxidase in Drosophila gut immunity. Science. 2005; 310:847–850. [PubMed: 16272120]
4. Ha EM, Oh CT, Ryu JH, et al. An antioxidant system required for host protection against gut infection in Drosophila. Developmental cell. 2005; 8:125–132. [PubMed: 15621536]
5. Chavez V, Mohri-Shiomi A, Garsin DA. Ce-Duox1/BLI-3 generates reactive oxygen species as a protective innate immune mechanism in Caenorhabditis elegans. Infection and immunity. 2009; 77:4983–4989. [PubMed: 19687201]
6. Flores MV, Crawford KC, Pullin LM, et al. Dual oxidase in the intestinal epithelium of zebrafish larvae has anti-bacterial properties. Biochemical and biophysical research communications. 2010; 400:164–168. [PubMed: 20709024]
7. Dupuy C, Ohayon R, Valent A, et al. Purification of a novel flavoprotein involved in the thyroid NADPH oxidase. Cloning of the porcine and human cdnas. The Journal of biological chemistry. 1999; 274:37265–37269. [PubMed: 10601291]
8. De Deken X, Wang D, Many MC, et al. Cloning of two human thyroid cDNAs encoding new members of the NADPH oxidase family. The Journal of biological chemistry. 2000; 275:23227–23233. [PubMed: 10806195]
9. Grasberger H, Refetoff S. Identification of the maturation factor for dual oxidase. Evolution of an eukaryotic operon equivalent. The Journal of biological chemistry. 2006; 281:18269–18272. [PubMed: 16651268]
10. El Hassani RA, Benfares N, Caillou B, et al. Dual oxidase2 is expressed all along the digestive tract. American journal of physiology Gastrointestinal and liver physiology. 2005; 288:G933–942. [PubMed: 15591162]
11. Csillag C, Nielsen OH, Vainer B, et al. Expression of the genes dual oxidase 2, lipocalin 2 and regenerating islet-derived 1 alpha in Crohn's disease. Scandinavian journal of gastroenterology. 2007; 42:454–463. [PubMed: 17454855]
12. Hamm CM, Reimers MA, McCullough CK, et al. NOD2 status and human ileal gene expression. Inflammatory bowel diseases. 2010; 16:1649–1657. [PubMed: 20155851]
13. Aerssens J, Camilleri M, Talloen W, et al. Alterations in mucosal immunity identified in the colon of patients with irritable bowel syndrome. Clinical gastroenterology and hepatology: the official clinical practice journal of the American Gastroenterological Association. 2008; 6:194–205. [PubMed: 18237869]
14. Hornsby MJ, Huff JL, Kays RJ, et al. Helicobacter pylori induces an antimicrobial response in rhesus macaques in a cag pathogenicity island-dependent manner. Gastroenterology. 2008; 134:1049–1057. [PubMed: 18395086]

15. Grasberger H, De Deken X, Mayo OB, et al. Mice deficient in dual oxidase maturation factors are severely hypothyroid. Molecular endocrinology. 2012; 26:481–492. [PubMed: 22301785]
16. Mohammadi M, Redline R, Nedrud J, et al. Role of the host in pathogenesis of Helicobacter-associated gastritis: H. felis infection of inbred and congenic mouse strains. Infection and immunity. 1996; 64:238–245. [PubMed: 8557346]
17. Danon SJ, O'Rourke JL, Moss ND, et al. The importance of local acid production in the distribution of Helicobacter felis in the mouse stomach. Gastroenterology. 1995; 108:1386–1395. [PubMed: 7729630]
18. Mazzucchelli L, Blaser A, Kappeler A, et al. BCA-1 is highly expressed in Helicobacter pylori-induced mucosa-associated lymphoid tissue and gastric lymphoma. The Journal of clinical investigation. 1999; 104:R49–54. [PubMed: 10562310]
19. Luzza F, Parrello T, Monteleone G, et al. Up-regulation of IL-17 is associated with bioactive IL-8 expression in Helicobacter pylori-infected human gastric mucosa. Journal of immunology. 2000; 165:5332–5337.
20. Every AL, Chionh YT, Skene CD, et al. Muc1 limits Helicobacter felis binding to gastric epithelial cells but does not limit colonization and gastric pathology following infection. Helicobacter. 2008; 13:489–493. [PubMed: 19166413]
21. Chen PR, Brugarolas P, He C. Redox signaling in human pathogens. Antioxidants & redox signaling. 2011; 14:1107–1118. [PubMed: 20578795]
22. Imlay JA. Cellular defenses against superoxide and hydrogen peroxide. Annual review of biochemistry. 2008; 77:755–776.
23. Stent A, Every AL, Sutton P. Helicobacter pylori defense against oxidative attack. American journal of physiology Gastrointestinal and liver physiology. 2012; 302:G579–587. [PubMed: 22194421]
24. Arnold IC, Zigova Z, Holden M, et al. Comparative whole genome sequence analysis of the carcinogenic bacterial model pathogen Helicobacter felis. Genome biology and evolution. 2011; 3:302–308. [PubMed: 21402865]
25. Huang CH, Chiou SH. Proteomic analysis of upregulated proteins in Helicobacter pylori under oxidative stress induced by hydrogen peroxide. The Kaohsiung journal of medical sciences. 2011; 27:544–553. [PubMed: 22208537]
26. Stewart PE, Carroll JA, Dorward DW, et al. Characterization of the Bat proteins in the oxidative stress response of Leptospira biflexa. BMC microbiology. 2012; 12:290. [PubMed: 23234440]
27. Halliwell B, Clement MV, Long LH. Hydrogen peroxide in the human body. FEBS letters. 2000; 486:10–13. [PubMed: 11108833]
28. Chavez V, Mohri-Shiomi A, Maadani A, et al. Oxidative stress enzymes are required for DAF-16-mediated immunity due to generation of reactive oxygen species by Caenorhabditis elegans. Genetics. 2007; 176:1567–1577. [PubMed: 17483415]
29. Harris AG, Wilson JE, Danon SJ, et al. Catalase (KatA) and KatA-associated protein (KapA) are essential to persistent colonization in the Helicobacter pylori SS1 mouse model. Microbiology. 2003; 149:665–672. [PubMed: 12634335]
30. Olczak AA, Seyler RW Jr, Olson JW, et al. Association of Helicobacter pylori antioxidant activities with host colonization proficiency. Infection and immunity. 2003; 71:580–583. [PubMed: 12496216]
31. Shin K, Yamauchi K, Teraguchi S, et al. Susceptibility of Helicobacter pylori and its urease activity to the peroxidase-hydrogen peroxide-thiocyanate antimicrobial system. Journal of medical microbiology. 2002; 51:231–237. [PubMed: 11871618]
32. Song Y, Driessens N, Costa M, et al. Roles of hydrogen peroxide in thyroid physiology and disease. The Journal of clinical endocrinology and metabolism. 2007; 92:3764–3773. [PubMed: 17666482]
33. Elfvin A, Edebo A, Bolin I, et al. Quantitative measurement of nitric oxide and hydrogen peroxide in Helicobacter pylori-infected Mongolian gerbils in vivo. Scandinavian journal of gastroenterology. 2007; 42:1175–1181. [PubMed: 17852850]

34. Schreiber S, Stuben M, Josenhans C, et al. In vivo distribution of Helicobacter felis in the gastric mucus of the mouse: experimental method and results. Infection and immunity. 1999; 67:5151–5156. [PubMed: 10496889]
35. Schreiber S, Konradt M, Groll C, et al. The spatial orientation of Helicobacter pylori in the gastric mucus. Proceedings of the National Academy of Sciences of the United States of America. 2004; 101:5024–5029. [PubMed: 15044704]
36. Seaver LC, Imlay JA. Alkyl hydroperoxide reductase is the primary scavenger of endogenous hydrogen peroxide in Escherichia coli. Journal of bacteriology. 2001; 183:7173–7181. [PubMed: 11717276]
37. Corcionivoschi N, Alvarez LA, Sharp TH, et al. Mucosal reactive oxygen species decrease virulence by disrupting Campylobacter jejuni phosphotyrosine signaling. Cell host & microbe. 2012; 12:47–59. [PubMed: 22817987]
38. Hyslop PA, Hinshaw DB, Scraufstatter IU, et al. Hydrogen peroxide as a potent bacteriostatic antibiotic: implications for host defense. Free radical biology & medicine. 1995; 19:31–37. [PubMed: 7635356]
39. Lipinski S, Till A, Sina C, et al. DUOX2-derived reactive oxygen species are effectors of NOD2-mediated antibacterial responses. Journal of cell science. 2009; 122:3522–3530. [PubMed: 19759286]
40. Finkel T. Signal transduction by reactive oxygen species. The Journal of cell biology. 2011; 194:7–15. [PubMed: 21746850]
41. Mishina NM, Tyurin-Kuzmin PA, Markvicheva KN, et al. Does cellular hydrogen peroxide diffuse or act locally? Antioxidants & redox signaling. 2011; 14:1–7. [PubMed: 20690882]
42. Miller EW, Dickinson BC, Chang CJ. Aquaporin-3 mediates hydrogen peroxide uptake to regulate downstream intracellular signaling. Proceedings of the National Academy of Sciences of the United States of America. 2010; 107:15681–15686. [PubMed: 20724658]
43. Niethammer P, Grabher C, Look AT, et al. A tissue-scale gradient of hydrogen peroxide mediates rapid wound detection in zebrafish. Nature. 2009; 459:996–999. [PubMed: 19494811]
44. Razzell W, Evans IR, Martin P, et al. Calcium flashes orchestrate the wound inflammatory response through DUOX activation and hydrogen peroxide release. Current biology: CB. 2013; 23:424–429. [PubMed: 23394834]
45. Luxen S, Belinsky SA, Knaus UG. Silencing of DUOX NADPH oxidases by promoter hypermethylation in lung cancer. Cancer research. 2008; 68:1037–1045. [PubMed: 18281478]
46. Juarez MT, Patterson RA, Sandoval-Guillen E, et al. Duox, Flotillin-2, and Src42A are required to activate or delimit the spread of the transcriptional response to epidermal wounds in Drosophila. PLoS genetics. 2011; 7:e1002424. [PubMed: 22242003]
47. Athanasiadou S, Jones LA, Burgess ST, et al. Genome-wide transcriptomic analysis of intestinal tissue to assess the impact of nutrition and a secondary nematode challenge in lactating rats. PloS one. 2011; 6:e20771. [PubMed: 21698235]
48. Eaton KA, Danon SJ, Krakowka S, et al. A reproducible scoring system for quantification of histologic lesions of inflammatory disease in mouse gastric epithelium. Comparative medicine. 2007; 57:57–65. [PubMed: 17348292]
49. Testerman TL, Conn PB, Mobley HL, et al. Nutritional requirements and antibiotic resistance patterns of Helicobacter species in chemically defined media. Journal of clinical microbiology. 2006; 44:1650–1658. [PubMed: 16672389]

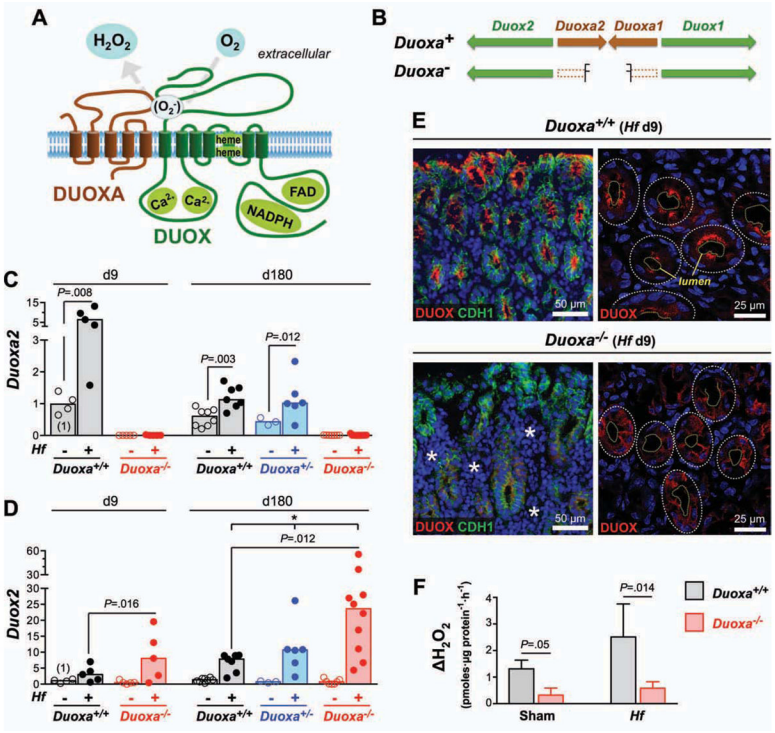

Fig. 1. *Hf* infection induces DUOX2 expression in the gastric surface epithelium

A) Topology model depicting the heterodimeric structure of a functional DUOX complex. B) Arrangement of DUOX and DUOXA subunit genes in mice (identical to other mammals). *Duoxa*$^{-}$ indicates *Duoxa*-deficient allele. C–D) RT-qPCR determination of *Duoxa2* (C) and *Duox2* (D) expression in the gastric corpus. Data points represent average expression values of individual mice. Bars indicate median expression values of N=5 to 11 mice per group. * P<.05 (Kruskal-Wallis test). E) Release of H_2O_2 from gastric glands isolated from *Hf* or mock-infected *Duoxa*$^{-/-}$ mice and wild type littermates. Extracellular H_2O_2 accumulation was calculated from the catalase-inhibitable change in signal in the fluorescence-based H_2O_2 assay, normalized for protein content in the gland preps. Data represent median and range of N=4 mice per group from two independent experiments. F) Immunostaining of DUOX proteins in the gastric epithelium of mice infected for 9 days with *Hf*. In *Duoxa*$^{-/-}$ mice, DUOX detection is limited to epithelial cells neighboring extensive E-cadherin (*CDH1*) negative infiltrates (*asterisks*). Confocal imaging (*right panels*) shows targeting of DUOX proteins to the apical surface in infected wild type but not *Duoxa*$^{-/-}$ animals. *Dashed lines*, lumen and circumference of individual glands.

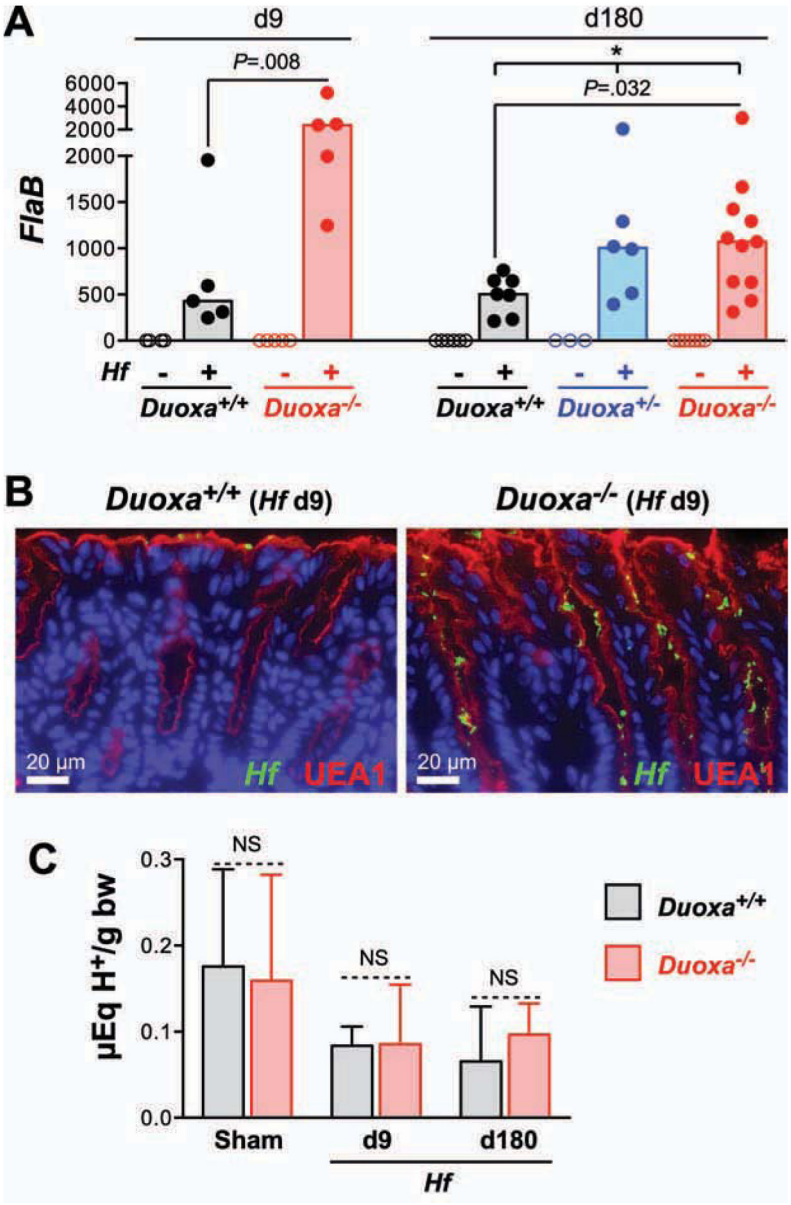

Fig. 2. Loss of functional DUOX enzymes leads to increased mucosal colonization by *Helicobacter*

A) Relative *Hf* colonization levels in the acute and chronic phase of infection determined by realtime qPCR. Expression of the *Hf* housekeeping gene *flaB* in gastric corpus samples was normalized for the amount of host mRNA (*Hprt1*). Bars indicate median values. * $P<.05$. B) Immunofluorescent detection of *Hf* in the gastric body at 9 days post infection. Mucus is visualized with *Ulex Europaeus* agglutinin 1 (UEA-1). C) Acidity of the gastric content expressed as µEq H^+ per gram of body weight. Data represent median and range of the acidity values of N=5 to 10 mice per group. *NS* $P>.05$.

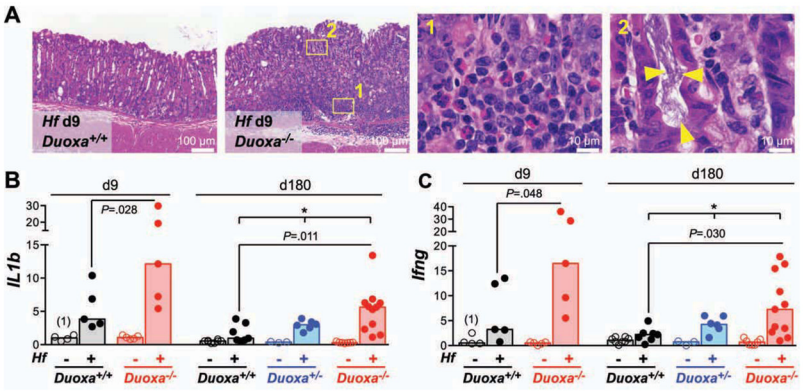

Fig. 3. *Hf*-induced acute gastritis is exacerbated in *Duoxa*$^{-/-}$ mice

A) Representative hematoxylin and eosin stained sections of the midcorpus 9 days post infection showing marked mixed-myeloid infiltrates in the mucosa and submucosa of infected *Duoxa*$^{-/-}$ mice compared to wild type controls. *Yellow triangles* indicate spiral shaped bacteria within a gastric gland. B–C) mRNA expression of acute inflammation markers interleukin-1β (B) and interferon-γ (C) in the midcorpus. Bars show median expression values of N=5 to 11 mice per group. * $P<.05$.

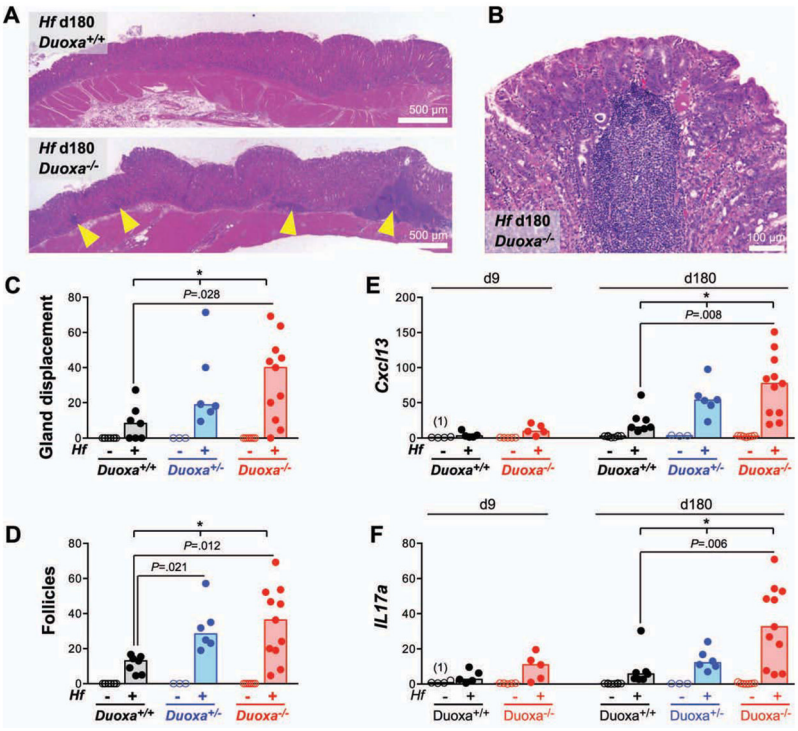

Fig. 4. Chronic follicular gastritis is more severe in *Duoxa*$^{-/-}$ mice

A–B) Histology at 6 months post infection depicting increased number of lymphoid aggregates in the gastric corpus of chronically infected *Duoxa*$^{-/-}$ mice. C–D) Histologic scoring of gland displacement (C) and frequency of lymphoid follicles (D). E–F) mRNA expression profiles of CXCL13 (E) and interleukin-17A (F). Bars represent medians. * $P<.05$.

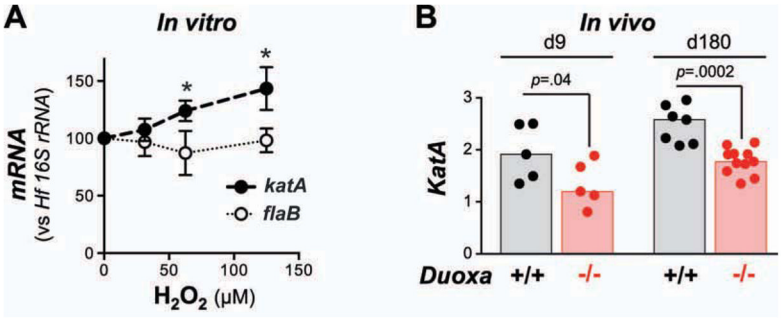

Fig. 5. *Hf* colonizing the gastric mucosa of *Duoxa*$^{-/-}$ mice express lower level of H_2O_2-inducible *katA* mRNA

A) H_2O_2 induces *Hf katA* expression in vitro. Bacteria were cultured for 12 h following addition of H_2O_2 at the indicated concentrations. Data represent mean ± standard deviation of the mean of three independent experiments. * $P<.05$. B) In vivo *katA* expression of *Hf* colonizing the gastric mucosa of wild type and *Duoxa*$^{-/-}$ animals, respectively. Data were normalized to the *Hf* housekeeping gene *flaB*. Bars depict median values of N=5 to 11 mice per group.

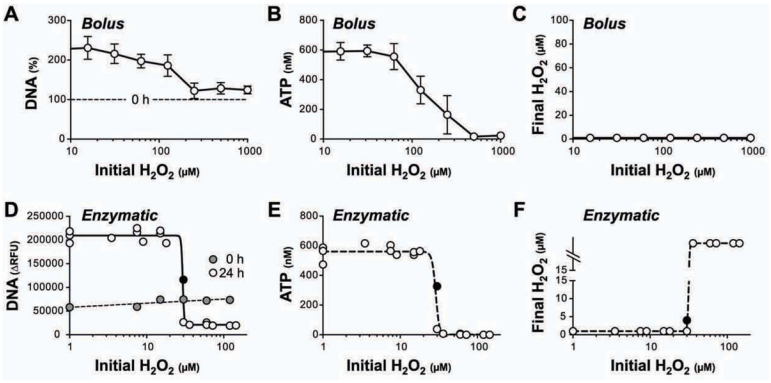

Fig. 6. *Hf* is susceptible to transient or sustained exposure to μM concentrations of H_2O_2

Bolus treatment: H_2O_2 was added to bacterial cultures (3.2×10^6 *Hf*/ml) at the indicated concentrations. Bacterial DNA (A) and intrabacterial ATP (B) level were determined following 18 h culture under microaerophilic conditions. Note that added H_2O_2 is completely scavenged by *Hf* resulting in transient exposure (C). *Enzymatic exposure:* For each experiment, *Hf* cultures (1.6×10^6 *Hf*/ml) were challenged with dilutions of glucose oxidase and cultured for 24 h. Results represent three independent experiments. Bacterial DNA (D) and ATP level (E) were measured at the end of the culture period. Values are plotted against the initial H_2O_2 equilibrium reached after glucose oxidase addition. H_2O_2 concentrations at the end of the culture period were either suppressed to background level of the medium (viable cultures; data points left to the critical threshold) or outside the measurement range (bacteria inactivated by accumulating H_2O_2; right to the transition). Note that the culture with 30 μM initial H_2O_2 level (*black filled symbol*) was closest to the equilibrium and had not fully outcompeted the oxidase activity at the end of the culture.